anti-inflammatory action without lowering blood glucose level in a rat model of type 1 diabetes. Diabetologia 54, 965-978, 2011
19) Sato C, Shikata K, Hirota D, Sasaki M, Nishishita S, Miyamoto S, Kodera R, Ogawa D, Tone A, Kataoka HU, Wada J, Kajitani N, Makino H. P-selectin glycoprotein ligand-1 deficiency is protective against obesity-related insulin resistance. Diabetes 60, 189-199, 2011
20) Kido Y, Ogawa D, Shikata K, Sasaki M, Nagase R, Okada S, Usui Kataoka HU, Wada J, Makino H. Intercellular adhesion molecule-1 plays a critical role in glomerulosclerosis after subtotal nephrectomy. Clin Exp Nephrol 15, 212-219, 2011
21) Miyatake N, Shikata K, Makino H, Numata T. Decreasing Abdominal Circumference Is Associated with Improving Estimated Glomerular Filtration Rate (eGFR) with Lifestyle Modification in Japanese Men:A Pilot Study. 1. Acta Med Okayama 65, 363-367, 2011
22) Tone A, Shikata K, Nakagawa K, Hashimoto M, Makino H. Renoprotective effects of clarithromycin via reduction of urinary MCP-1 levels in type 2 diabetic patients. Clin Exp Nephrol 15, 79-85, 2011
23) Miyatake N, Shikata K, Makino H, Numata T. The Relation between estimated glomerular filtration rate (eGFR) and proteinuria in Okayama prefecture, Japan. Environ Health Prev Med 16, 191-195, 2011
24) Miyatake N, Shikata K, Makino H, Numata T. Comparison of ventilatory threshold between subjects with and without proteinuria in Japanese. Health 3, 6, 394-399, 2011
25) Miyatake N, Shikata K, Makno H, Numata T. Decreasing serum uric acid levels might be associated with improving estimated glomerular filtration rate (eGFR) in Japanese men. Health 3, 8, 498-503, 2011
26) Miyatake N, Nishii K, Numata T. Relationship between work style and cigarette smoking in Japanese workers. Health 3, 9, 537-541, 2011
27) Miyatake N, Shikata K, Makino H, Numata T. The relation between estimated glomerular filtration rate (eGFR) and coffee consumption in the Japanese. Health 3, 9, 549-552, 2011
28) Miyatake N, Shikata K, Makino H, Numata T. Comparison of muscle strength between subjects with and without proteinuria. Health 3, 11, 698-702, 2011
29) 原章規・和田隆志: Q25.AAVの寛解、再燃の定義を教えてください. 急速進行性糸球体腎炎 診療ガイドQ&A, 診断と治療社 , 2011
30) 原章規・和田隆志: Q24.RPGNの寛解、再燃の定義を教えてください. 急速進行性糸球体腎炎 診療ガイドQ&A, 診断と治療社 , 2011
31) 原章規・和田隆志: 7.ドーパミンは、どんな場合にどのように使うのでしょうか? EBM 腎臓病の治療, 中外医学社 , 2011
32) 和田隆志: 糖尿病性腎症. 今日の治療指針 2012, 医学書院 東京, 2012
33) 原章規・和田隆志. 糖尿病性腎症の進展におけるケモカインーケモカイン受容体の役割. 日本腎臓学会誌 53 (7), 1027-1033, 2011
34) Hara A, Sakai N, Wada T. Pathogenesis of diabetic complications through bone marrow-derived cells. Journal of Wound Technology in press

35) 和田隆志. 糖尿病性腎症. 月刊　カレントテラピー 29 (8) , 666-670, 2011
36) Wada T, Sakai N, Sakai Y, Matsushima K, Kaneko S, Furuichi K. Involvement of bone-mar r ow-derived cells in kidney fibrosis. Clin Exp Nephrol 15, 8-13, 2011
37) Shimizu K, Furuichi K, Sakai N, Kitagawa K, Matsushima K, Mukaida N, Kaneko S, Wada T. Fractalkine and its receptor, CX3CR1, promote hypertensive interstitial fibrosis in the kidney. Hypertens Res 34, 747-752, 2011
38) Wada T, Shimizu M, Toyama T, Hara A, Kaneko S, Furuichi K. Clinical impact of albuminuria in diabetic nephropathy. Clin Exp Nephrol , , 2011
39) Nakade Y, Takamura T, Sakurai M, Misu H, Nagata M, Nanbu Y, Oe H, Takamura T, Sakai Y, Kaneko S, Wada T. Association between coefficients of variation of the R-R intervals on electrocardiograms and post-challenge hyperglycemia in patients with newly diagnosed type2 diabetes. J Diabetes Invest 2(4), 324-327, 2011
40) Kokubo S, Sakai N, Furuichi K, Toyama T, Kitajima S, Okumura T, Matsushima K, Kaneko S, Wada T. Activation of p38 mitogen-activated protein kinase promotes peritoneal fibrosis by regulating fibrocytes. Perit Dial Int, 2011
41) Ito M, Sugihara K, Asaka T, Toyama T, Yoshihara T, Furuichi K, Wada T, Asano M. Glycoprotein Hyposialylation Gives Rise to a Nephrotic-Like Syndrome That Is Prevented by Sialic Acid Administration in GNE V572L Point-Mutant Mice. PLoS ONE 7(1), 1-13, 2011
42) Furuichi K, Kokubo S, Hara A, Imamura R, Wang Q, Kitajima S, Toyama T, Okumura T, Matsushima K, Suda T, Mukaida N, Kaneko S, Wada T. Fas ligand has a greater impact than TNF-α on apoptosis and inflammation in ischemic acute kidney injury. Nephron Extra 2, 27-38, 2012
43) Furuichi K, Shintani H, Sakai Y, Ochiya T, Matsushima K, Kaneko S, Wada T. Effects of Adipose-Derived Mesenchymal Cells on Ischemia-Reperfusion Injury in Kidney. Clin Exp Nephrol in press 2012

# 研究成果の刊行物・別刷

# Decreased renal α-Klotho expression in early diabetic nephropathy in humans and mice and its possible role in urinary calcium excretion

Osamu Asai[1], Kimihiko Nakatani[1,2], Tomohiro Tanaka[3], Hirokazu Sakan[1], Akihiro Imura[3], Shuhei Yoshimoto[1], Ken-ichi Samejima[1], Yukinari Yamaguchi[1], Masaru Matsui[1], Yasuhiro Akai[1], Noboru Konishi[2], Masayuki Iwano[1,4], Yoichi Nabeshima[3] and Yoshihiko Saito[1,5]

*[1]First Department of Internal Medicine, Nara Medical University, Kashihara, Japan; [2]Department of Pathology, Nara Medical University, Kashihara, Japan; [3]Department of Pathology and Tumor Biology, Kyoto University Graduate School of Medicine, Kyoto, Japan; [4]Division of Nephrology, Department of General Medicine, Faculty of Medical Sciences, University of Fukui, Yoshida-gun, Japan and [5]Department of Regulatory Medicine for Blood Pressure, Nara Medical University, Kashihara, Japan*

**Hypercalciuria is one of the early manifestations of diabetic nephropathy. We explored here the role of α-Klotho, a protein expressed predominantly in distal convoluted tubules that has a role in calcium reabsorption. We studied 31 patients with early diabetic nephropathy and compared them with 31 patients with IgA nephropathy and 7 with minimal change disease. Renal α-Klotho expression was significantly lower and urinary calcium excretion (UCa/UCr) significantly higher in diabetic nephropathy than in IgA nephropathy or minimal change disease. Multiple regression analyses indicated that α-Klotho mRNA was inversely correlated with calcium excretion. We next measured these parameters in a mouse model of streptozotocin (STZ)-induced diabetic nephropathy, characterized by glomerular hyperfiltration, as seen in early diabetic nephropathy. We also confirmed a reduction of renal α-Klotho mRNA down to almost 50% and enhanced calcium excretion in mice with STZ-induced diabetic nephropathy in comparison with nondiabetic mice. Hypercalciuria was exacerbated in heterozygous α-Klotho knockout mice in comparison with wild-type mice, each with STZ-induced diabetic nephropathy. Thus, α-Klotho expression was decreased in distal convoluted tubules in diabetic nephropathy in humans and mice. Renal loss of α-Klotho may affect urinary calcium excretion in early diabetic nephropathy.**

*Kidney International* advance online publication, 4 January 2012; doi:10.1038/ki.2011.423

KEYWORDS: diabetic nephropathy; hypercalciuria; hypoxia

**Correspondence:** *Kimihiko Nakatani, First Department of Internal Medicine, Nara Medical University, 840, Shijo-cho, Kashihara, Nara, 634-8522, Japan. E-mail: nkimihik@naramed-u.ac.jp*

**Received 9 March 2011; revised 28 September 2011; accepted 11 October 2011**

Hypercalciuria is one of the early findings of uncontrolled diabetes mellitus in both humans and experimental animal models.[1–4] Hypercalciuria is essentially associated with a negative calcium balance hallmarked by renal calcium loss in diabetes mellitus,[1,2] which has been proposed to contribute to the increased risk of bone fracture.[5,6] Although osmotic diuresis and increased dietary calcium intake secondary to hyperphagia may have a role in the hypercalciuria seen in diabetic patients,[2] control of osmotic diuresis with appropriate insulin therapy only partially corrects hypercalciuria.[7] Furthermore, increased dietary calcium intake may not increase the calcium load on the kidney, because calcium absorption in the gut is also decreased in the early stages of streptozotocin (STZ)-induced diabetes.[8,9] Thus, there may be impairment in the renal handling of calcium in diabetes mellitus. Although ultrafiltered calcium is reabsorbed in the proximal tubules and the distal convoluted tubules (DCTs),[10] previous studies have not revealed any decreases in calcium reabsorption in the proximal tubules in diabetic models.[7,11,12] Thus, DCTs may contribute to the impairment in calcium transport,[7] the underlying molecular mechanisms of which remain unclear.

α-Klotho (α-KL) mutant mice were originally used to model disorders associated with human aging, because the phenotype of the mutant animals includes arteriosclerosis, ectopic calcification (including vascular calcification), emphysema, and osteoporosis.[13] The *α-KL* gene is predominantly expressed in the parathyroid glands, the DCTs in the kidney, and the choroid plexus in the brain,[14,15] all of which have an important role in calcium–phosphorus homeostasis. Recently, evidence has accumulated showing that α-KL regulates (1) parathyroid hormone (PTH) release in the parathyroid gland,[14] (2) the production of $1,25(OH)_2$ vitamin $D_3$ by negatively regulating the expression of 1α-hydroxylase, which encodes a rate-limiting enzyme of active vitamin D synthesis,[16,17] and (3) transepithelial calcium transport in the

DCTs via activation of the transient receptor potential vanilloid 5 (TRPV5) channel.[18] In fact, mice lacking α-KL display diminished renal calcium reabsorption, resulting in severe hypercalciuria.[19]

In this study, we showed that renal α-KL expression levels were decreased in patients with early diabetic nephropathy (DN) and in the STZ-induced mouse model of diabetes, and that renal α-KL expression levels were inversely correlated with urinary calcium augmentation in patients with DN and a mouse model of DN. Furthermore, we confirmed the exaggerated urinary excretion of calcium in STZ-induced DN in heterozygous α-KL knockout mice (α-KL$^{+/-}$ mice). Thus, we propose that renal α-KL expression levels are partially involved in hypercalciuria in early DN.

## RESULTS

### Elevation of urinary calcium excretion (UCa/UCr) in patients with DN

Urinary calcium excretion (UCa/UCr), which was normalized to the urinary creatinine, was significantly higher in patients with DN than in those with either IgA nephropathy (IgAN) or minimal change disease (MCD) (DN, 0.081 ± 0.044; IgAN, 0.037 ± 0.021; MCD, 0.039 ± 0.022; $P<0.001$; Figure 1a). Serum calcium concentrations were similar among the three patient groups (Table 1). On considering the population subset with an estimated glomerular filtration rate (eGFR) greater than 60 ml/min per 1.73 m$^2$, UCa/UCr levels in DN were highly elevated relative to those seen in

**Table 1 | Clinical characteristics of study population**

| | DN | IgAN | MCD |
|---|---|---|---|
| Number of patients | 74 | 90 | 26 |
| Age (years) | 64 ± 10† | 40 ± 16 | 35 ± 16 |
| Serum creatinine (mg/dl) | 0.95 ± 0.48 | 0.85 ± 0.31 | 0.82 ± 0.22 |
| eGFR (ml/min per 1.73 m$^2$)[a] | 74.4 ± 24.9 | 79.2 ± 23.9 | 87.2 ± 22.5‡ |
| Corrected serum calcium (mg/dl) | 9.4 ± 0.4 | 9.3 ± 0.3 | 9.5 ± 0.4 |

Abbreviations: DN, diabetic nephropathy; eGFR, estimated glomerular filtration rate; IgAN, IgA nephropathy; MCD, minimal change disease.
Clinical parameters are presented as means ± s.d.
[a]eGFR was calculated by means of the creatinine-based Modification of Diet in Renal Disease Study Equation. †$P<0.05$ vs. IgAN or MCD. ‡$P<0.05$ vs. DN.

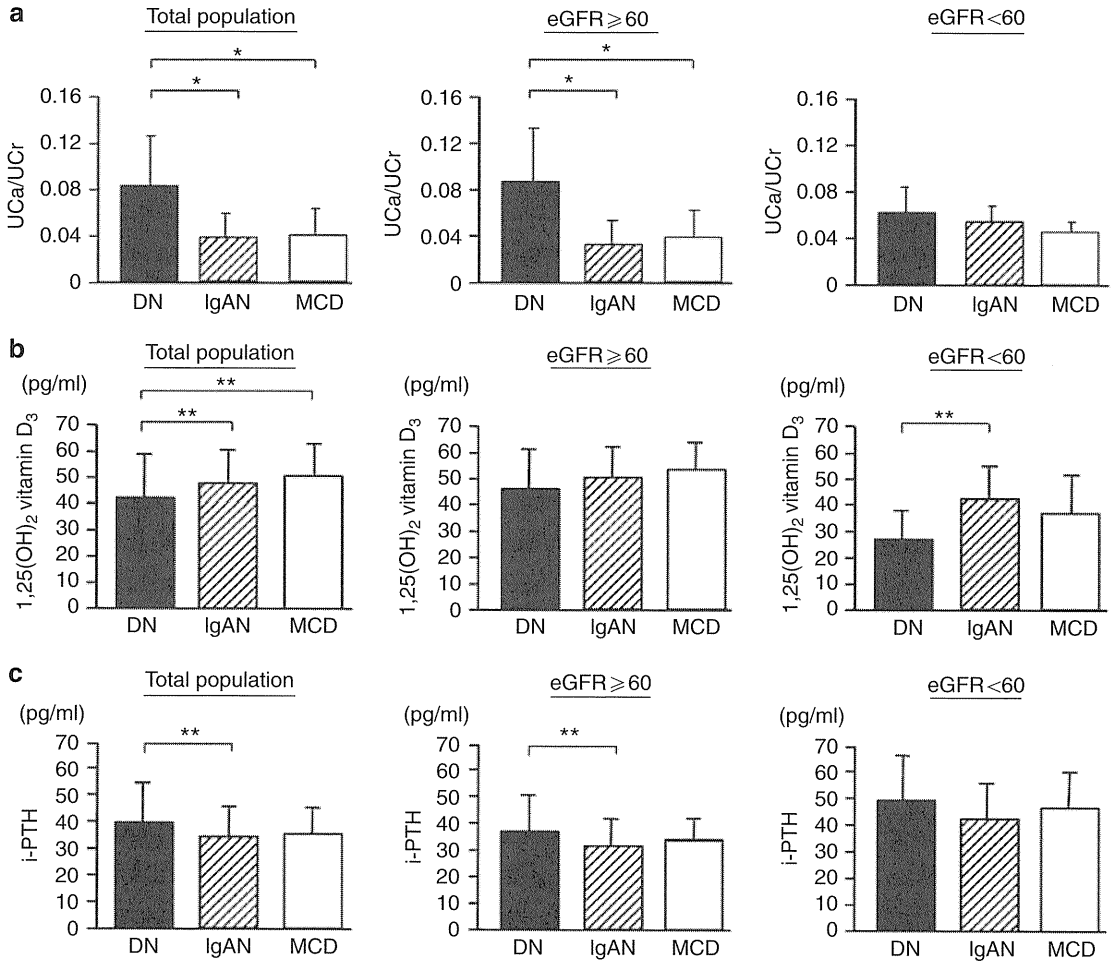


**Figure 1 | Elevation of urinary calcium excretion (UCa/UCr) in patients with diabetic nephropathy (DN).** (**a**) UCa/UCr, (**b**) serum 1,25(OH)$_2$ vitamin D$_3$ concentration, and (**c**) serum intact parathyroid hormone (i-PTH) concentration were measured in patients with DN (black bars), IgA nephropathy (IgAN) (striped bars), or minimal change disease (MCD) (white bars). Data are shown as means ± s.e.m. for each group. Kruskal–Wallis analysis of variance by ranks with Bonferroni adjustment was used to compare groups. *$P<0.001$; **$P<0.01$.

IgAN and MCD (DN, 0.086 ± 0.047; IgAN, 0.032 ± 0.020; MCD, 0.038 ± 0.024; $P<0.001$; Figure 1a). In patients with an eGFR under 60 ml/min per 1.73 $m^2$, however, there was no significant difference in UCa/UCr levels between DN, IgAN, and MCD (DN, 0.062 ± 0.021; IgAN, 0.054 ± 0.013; MCD, 0.045 ± 0.009; $P=0.265$; Figure 1a). Serum levels of 1,25$(OH)_2$ vitamin $D_3$ were significantly lower in DN than in IgAN and MCD (DN, 41.69 ± 16.1 pg/ml; IgAN, 48.18 ± 12.51 pg/ml; MCD, 50.2 ± 12.6 pg/ml; $P=0.004$; Figure 1b). In the population with an eGFR greater than 60 ml/min per 1.73 $m^2$, however, serum 1,25$(OH)_2$ vitamin $D_3$ levels were lower in DN, as compared with IgAN and MCD, but this decrease was not significant (DN, 45.86 ± 14.88 pg/ml; IgAN, 50.00 ± 11.87 pg/ml; MCD, 52.61 ± 10.95 pg/ml; $P=0.069$; Figure 1b). Serum intact PTH (i-PTH) values were significantly increased in DN in comparison with those in IgAN for both the total study population (DN, 39.2 ± 15.19 pg/ml; IgAN, 33.68 ± 11.79 pg/ml; MCD, 35.23 ± 9.96 pg/ml; $P=0.027$, Figure 1c) and the population subset with an eGFR greater than 60 ml/min per 1.73 $m^2$ (DN, 36.53 ± 13.65 pg/ml; IgAN, 31.16 ± 10.20 pg/ml; MCD, 33.09 ± 7.99 pg/ml; $P=0.032$; Figure 1c).

**Reduction in α-KL expression in the early stages of human DN**

In immunohistological examination, although α-KL reactivity was detectable exclusively in DCTs in patients with MCD and IgAN (Figure 2b and c), the reactivity was significantly reduced in samples from DN patients (Figure 2a). α-KL reactivity was also detected in the proximal convoluted tubules, although the reactivity in proximal convoluted tubules was weaker than that in DCTs. α-KL immunoreactivity in proximal convoluted tubules was similar to that in DN, IgAN, and MCD. Renal α-KL mRNA expression levels, quantitatively measured by real-time PCR, were significantly correlated with eGFR ($r=0.353$, $P=0.0034$; Figure 2e), suggesting that renal α-KL mRNA expression levels were decreased with the advance of renal failure. Notably, looking at the population with an eGFR greater than 60 ml/min per 1.73 $m^2$, renal α-KL mRNA expression levels were markedly decreased in the presence of DN in comparison with IgAN and MCD (DN, 0.45 ± 0.27 AU; IgAN, 1.07 ± 0.45 AU; MCD, 1.29 ± 0.58 AU; $P=0.0004$; Figure 2f). However, in the population subset with an eGFR under 60 ml/min per 1.73 $m^2$, renal α-KL mRNA expression levels were similar to those in DN, IgAN, and MCD (Figure 2f).

Next, we used the same renal biopsy specimens to investigate the degree of renal tubulointerstitial damage progression in the DN, IgAN, and MCD groups. Neither the average numbers of CD31-positive peritubular capillaries (PTCs) nor the percentage of type I collagen–positive areas per single field in DN were significantly different from those seen in IgAN or MCD when the eGFR was greater than

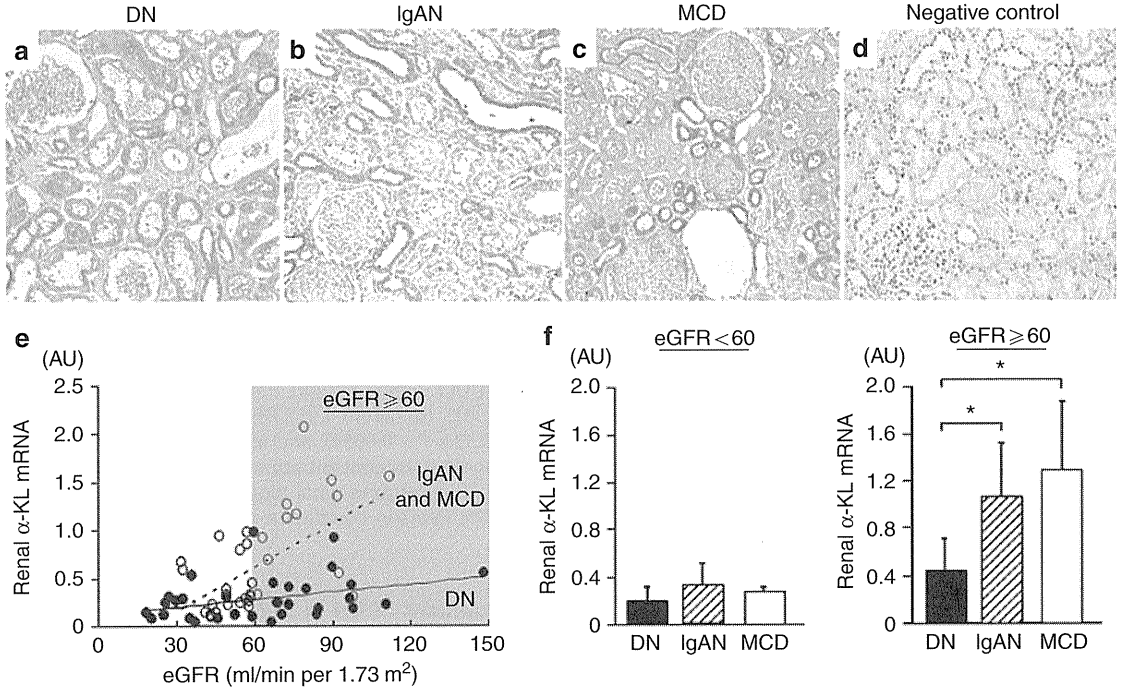


**Figure 2 | Reduction in α-Klotho (α-KL) expression in human early diabetic nephropathy (DN).** (**a**–**d**) Representative immunoperoxidase staining for α-KL protein in renal biopsy sections from human patients with DN, IgA nephropathy (IgAN), or minimal change disease (MCD), and negative control (MCD treated with rat immunoglobulins instead of rat anti-α-KL antibody). Original magnification, × 100. (**e**) Correlation of renal α-KL mRNA expression levels with estimated glomerular filtration rate (eGFR) in patients with DN (closed circles) and IgAN and MCD (open circles). (**f**) Renal α-KL mRNA expression levels in DN (black bars), IgAN (striped bars), and MCD (white bars). Data are shown as means ± s.e.m. for each group. Kruskal–Wallis analysis of variance by ranks with Bonferroni adjustment was used to compare groups. *$P<0.01$.

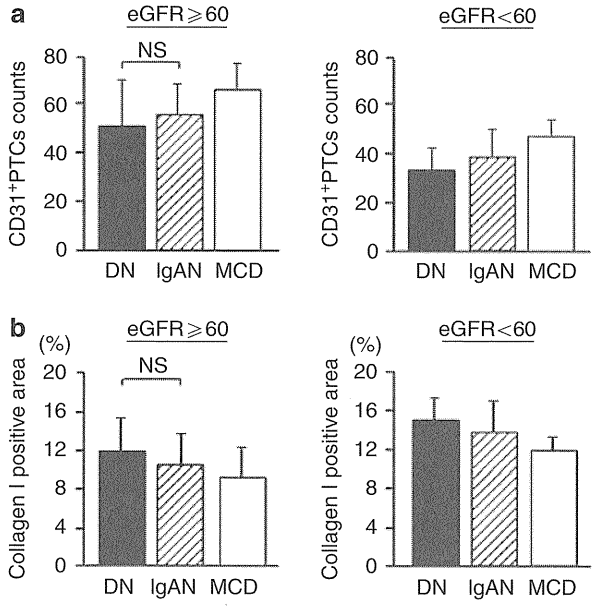


**Figure 3 | The degree of renal tubulointerstitial damage progression in the diabetic nephropathy (DN), IgA nephropathy (IgAN), and minimal change disease (MCD).** (**a**) The average number of CD31-positive peritubular capillaries (PTCs) and (**b**) the average proportion of type I collagen-positive areas per field in renal biopsy specimens from patients with DN (black bars), IgAN (striped bars), and MCD (white bars). Data are shown as means ± s.e.m. for each group. Kruskal–Wallis analysis of variance by ranks with Bonferroni adjustment was used to compare groups.

60 ml/min per 1.73 $m^2$ (CD31-positive PTC numbers: DN, 50.6 ± 18.9; IgAN, 55.2 ± 12.8; MCD, 66.8 ± 10.6; $P = 0.174$; Figure 3a; Type I collagen positive areas: DN, 11.7 ± 3.5%, IgAN 10.4 ± 3.2%, MCD 8.7 ± 3.2%; $P = 0.234$; Figure 3b).

### Correlation of renal α-KL mRNA expression levels with UCa/Ucr

An examination of three clinical parameters governing calcium metabolism—levels of renal α-KL expression, serum 1,25$(OH)_2$ vitamin $D_3$, and serum i-PTH—showed that levels of renal α-KL mRNA expression ($r = -0.642$, $P < 0.0001$), serum 1,25$(OH)_2$ vitamin $D_3$ ($r = -0.334$ $P = 0.0054$), and serum i-PTH ($r = 0.274$, $P = 0.0244$) correlated significantly with UCa/UCr across all patients with DN, IgAN, and MCD, who had undergone renal biopsy (Figure 4). Multiple regression analyses revealed that renal α-KL expression levels were significantly and inversely correlated with UCa/UCr ($\beta = 10.644$, $P < 0.0001$) as an independent variable in order of importance ($R^2 = 0.375$, $P < 0.0001$), but serum 1,25$(OH)_2$ vitamin $D_3$, serum i-PTH, serum calcium, eGFR, and age were not (Table 2), among all patients who had undergone renal biopsy. In patients with an eGFR greater than 60 ml/min per 1.73 $m^2$, univariate analysis showed that renal α-KL mRNA expression levels correlated significantly with only UCa/UCr ($r = -0.755$, $P < 0.0001$; data not shown).

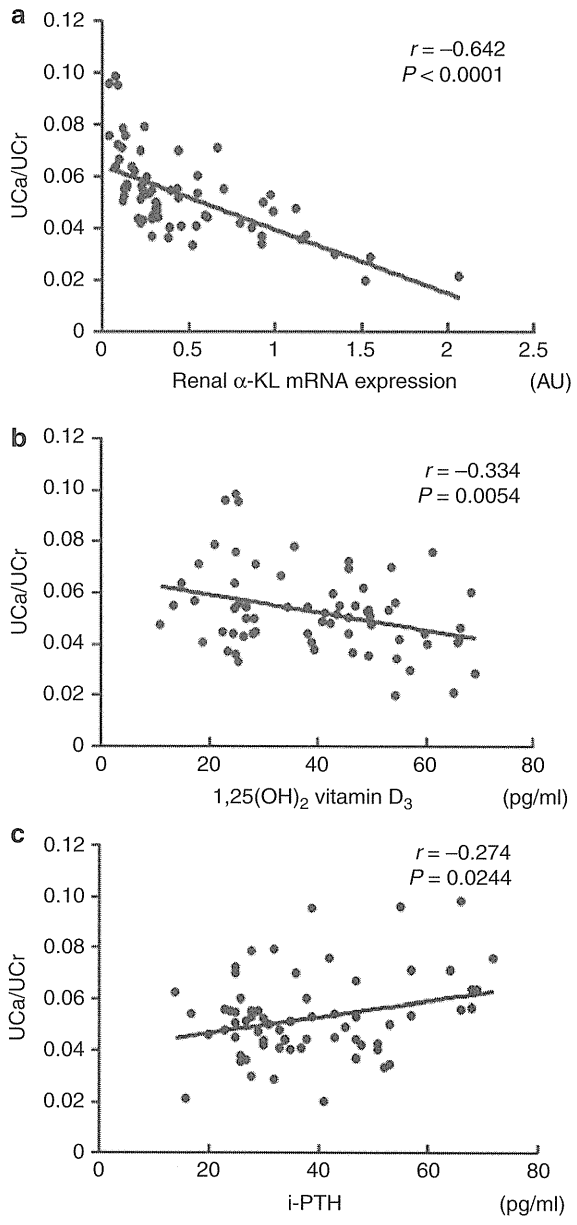


**Figure 4 | Correlation of renal α-Klotho (α-KL) mRNA expression levels with urinary calcium excretion (UCa/UCr).** (**a**) UCa/UCr with renal α-KL mRNA expression indices ($r = -0.642$, $P < 0.0001$), (**b**) serum 1,25$(OH)_2$ vitamin $D_3$ concentrations ($r = -0.334$, $P = 0.0054$), and (**c**) serum intact-parathyroid hormone (i-PTH) concentrations ($r = 0.274$, $P = 0.0244$) in patients who had undergone renal biopsy. Correlations were evaluated using the Pearson correlation coefficient.

### Development of DN in STZ-treated mice

In this human study, we revealed a significant decrease in renal α-KL expression levels and an increase in UCa/UCr in DN with an eGFR greater than 60 ml/min per 1.73 $m^2$. Therefore, to confirm that renal α-KL expression levels were decreased in early DN, and that this decrease was related to elevations in UCa/UCr, we used the STZ-induced mouse model of diabetes. In this model mouse, urinary albumin to creatinine ratios were increased at 2, 4, 6, and 8 weeks after

**Table 2 | Multiple regression analysis[a] for urinary calcium excretion (UCa/UCr)**

| Independent variable | $\beta^{\dagger}$ | *P*-value |
|---|---|---|
| Renal α-Klotho expression levels | −0.644 | <0.0001 |
| Serum 1,25(OH)$_2$ vitamin D$_3$ | 0.048 | 0.7131 |
| Serum intact-PTH | 0.151 | 0.1952 |
| eGFR | 0.05 | 0.7207 |
| Corrected serum calcium | −0.035 | 0.7268 |
| Age | 0.047 | 0.6961 |

Abbreviations: eGFR, estimated glomerular filtration rate; PTH, parathyroid hormone; UCa/UCr, urinary calcium (mg/dl)/urinary creatinine (mg/dl).
[a]Adjusted coefficient of determination ($R^2$); $R^2$=0.375, $P<0.0001$.
[†]Standard partial regression coefficient.

the establishment of diabetes (Supplementary Figure S1 online). This diabetic mouse model did not show apparent histopathological findings characteristic with DN at 8 weeks after the establishment of diabetes, indicating to be a useful model for early DN (Supplementary Figure S2 online).

### Decrease in renal α-KL expression levels and elevation of UCa/UCr in STZ-induced diabetic mice

In STZ-induced diabetic mice, renal α-KL mRNA expression levels were maintained until 4 weeks after the establishment of diabetes mellitus, but they decreased significantly to about 70% of the levels of nondiabetic control mice at 6 weeks and to about 50% at 8 weeks ($P<0.001$, Figure 5c). This decrease was also confirmed at the protein level by immunohistological examination and western blotting (Figure 5a and b). UCa/UCr in diabetic mice was slightly but significantly increased beginning 2 weeks after the establishment of diabetes mellitus, and it was further elevated at 6 and 8 weeks ($P<0.001$; Figure 5d). Interestingly, the levels of UCa/UCr in diabetic mice at 6 weeks significantly increased to about one and a half times as much as those in diabetic mice at 4 weeks, and these levels at 8 weeks showed a further significant increase to about two times as much as those at 4 weeks (Figure 5d). Thus, the reduction of renal α-KL expression in STZ-induced diabetic mice may be related to further enhancement of UCa/UCr levels.

### Exaggeration of UCa/UCr in STZ-induced diabetic α-KL$^{+/-}$ mice

To confirm whether or not the approximately 50% reduction in renal α-KL expression resulted in an elevation in UCa/UCr, we measured this excretion in α-KL$^{+/-}$ mice. There were no significant differences in UCa/UCr levels between α-KL$^{+/-}$ and α-KL$^{+/+}$ mice (Figure 6a). Next, we examined STZ-induced DN in α-KL$^{+/-}$ mice. To avoid the DN-related decline of renal α-KL expression, we examined UCa/UCr beginning 2 weeks after the establishment of diabetes mellitus in both diabetic α-KL$^{+/+}$ and α-KL$^{+/-}$ mice. During the first 2 weeks, although renal α-KL expression levels were similar in diabetic and nondiabetic mice of both genotypes (Figure 6b and c), UCa/UCr levels in diabetic α-KL$^{+/-}$ mice increased to about one and a half times as much as those in

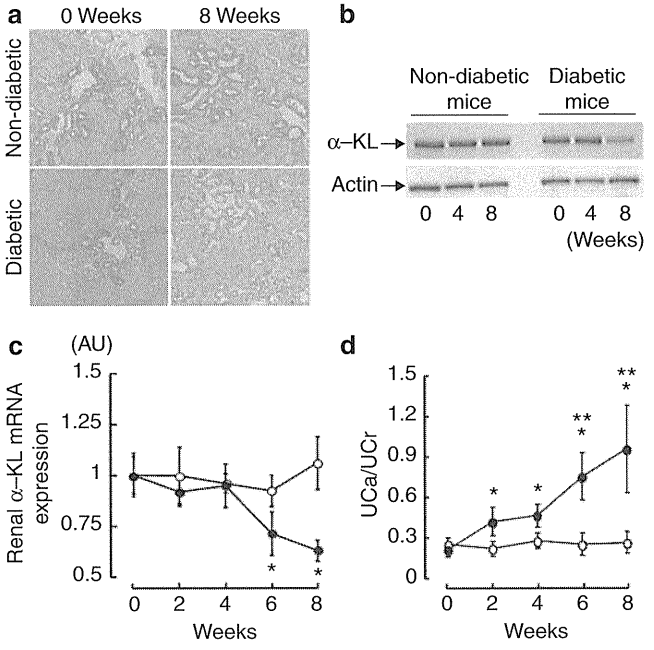


**Figure 5 | Decrease in renal α-Klotho (α-KL) expression levels and elevation of urinary calcium excretion (UCa/UCr) in streptozotocin (STZ)-induced diabetic mice.** (**a**) Representative immunoperoxidase staining for α-KL in kidney specimens, and (**b**) western blotting to detect α-KL of the kidney from the indicated mice. (**c**) Time course of renal α-KL mRNA expression levels and (**d**) time course of the urinary calcium (mg/dl) to creatinine (mg/dl) ratio in diabetic (closed circles) and nondiabetic (open circles) mice. Original magnification, × 100. Student's *t*-test was used to compare groups. *$P<0.001$, vs. nondiabetic mice; **$P<0.05$, vs. STZ-treated mice 4 weeks after the establishment of diabetes.

diabetic α-KL$^{+/+}$ mice ($P<0.001$; Figure 6a). Thus, when diabetes was induced, the 50% reduction in renal α-KL expression may be related to the greater increases in UCa/UCr levels in α-KL$^{+/-}$ mice than those in α-KL$^{+/+}$ mice.

### The effect of α-KL expression levels on the activity of TRPV5

TRPV5 is predominantly involved in renal calcium handling. TRPV5 colocalizes with α-KL in DCTs, and its activity is stimulated by α-KL.[18] Therefore, to investigate the mechanism by which the reduction of renal α-KL expression is related to the increase of urinary calcium excretion, we studied the effect of α-KL expression on TRPV5 activity. First, we verified that the level of renal TRPV5 expression was not significantly lower in DN with an eGFR greater than 60 ml/min per 1.73 m$^2$ than in IgAN or MCD, and also not lower in STZ-induced diabetic mice at 8 weeks than nondiabetic mice (Figure 7a–d), indicating that there is no significant association between the levels of α-KL expression and those of TRPV5 expression in the kidney. Next, to clarify whether or not TRPV5 channel activity is associated with the level of α-KL expression, we transfected both TRPV5 and various amounts of adenoviral vectors carrying the α-*KL* gene into human embryonic kidney 293 (HEK293) cells, and then

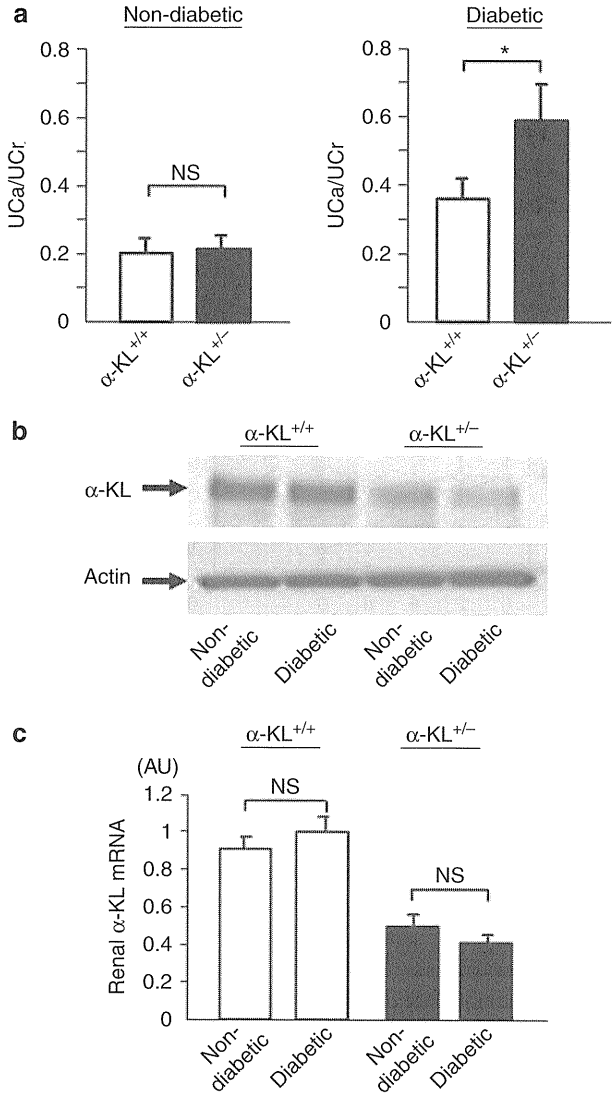


**Figure 6 | Exaggeration of urinary calcium excretion (UCa/UCr) in streptozotocin (STZ)-induced diabetic α-Klotho (α-KL)$^{+/-}$ mice.** (**a**) UCa/UCr in diabetic and nondiabetic mice of α-KL$^{+/-}$ (black bars) and α-KL$^{+/+}$ (white bars) strains. (**b**) Western blotting for α-KL in kidney specimens from the indicated mice, and (**c**) renal α-KL mRNA expression indices in diabetic and nondiabetic mice of α-KL$^{+/-}$ (black bars) and α-KL$^{+/+}$ (white bars) strains. Student's *t*-test was used to compare groups. *$P<0.001$.

analyzed calcium uptake in the transfectants. In this *in vitro* experiment, we showed that, in HEK293 transfected with both *TRPV5* and *α-KL* gene, calcium uptake was significantly increased in proportion to the α-KL expression (Figure 7e). In this experiment, HEK293 cells transfected with both *TRPV5* and *Lac Z* gene served as the control. We also found that calcium uptake did not significantly increase in HEK293 cells in the absence of TRPV5, even when α-KL expression was elevated (Figure 7e).

## DISCUSSION

This study demonstrated, for the first time, that renal α-KL expression levels in patients with DN were markedly decreased in comparison with those in patients with either IgAN or MCD with an eGFR greater than 60 ml/min per 1.73 m$^2$. We confirmed that UCa/UCr in patients with DN was markedly increased in comparison with patients with IgAN or MCD, and renal α-KL expression levels correlated significantly with UCa/UCr in humans. In the STZ-induced mouse model of diabetes, we also observed that the decreases in renal α-KL expression levels correlated with greater enhancement of UCa/UCr. Moreover, we confirmed the exacerbated renal calcium loss in KL$^{+/-}$ mice with STZ-induced DN. These findings indicate for the first time a significant correlation between renal α-KL loss and hypercalciuria in early DN.

Our study revealed that renal α-KL expression levels were significantly decreased in patients of DN with an eGFR greater than 60 ml/min per 1.73 m$^2$. Although eGFR is grossly related to the degree of renal tubulointerstitial damage, eGFR may not always be correlated with renal tubulointerstitial damage because of the development of glomerular hyperfiltration in the early stages of DN.[20,21] To exclude the possibility that increased tubulointerstitial damage was responsible for the observed decreases in renal α-KL expression in DN, we immunohistologically investigated PTC counts and the degree of interstitial fibrosis.[22,23] In the population of patients with an eGFR greater than 60 ml/min per 1.73 m$^2$, we did not observe any significant histological differences in tubulointerstitial damage among DN, IgAN, and MCD specimens. In addition to human examination, we confirmed the reduced expression of α-KL mRNA in the kidneys of STZ-induced diabetic mice, in which apparent glomerular and tubulointerstitial injury were not detected. These results suggest that a reduction of renal α-KL expression in the early stages of DN is a characteristic finding of DN.

Hypercalciuria is also an early finding characteristic of patients with DN,[1] and renal tubular calcium excretion is indicated to be increased in STZ-induced diabetes mellitus, despite exhibiting normal plasma calcium concentrations.[2–4] The precise mechanism of hypercalciuria in DN, however, remains unclear. In the present study, multiple regression analyses clearly showed that the renal expression of α-KL mRNA is an independent determinant of UCa/UCr, and the reduction of renal α-KL expression in STZ-induced diabetic mice was shown to enhance the diabetes-related increase of UCa/UCr levels. Thus, it is possible that the decline of α-KL mRNA in DCTs is responsible for the increase of UCa/UCr observed in DN. Given the evidence that α-KL$^{-/-}$ mice showed a tremendous increase in UCa/UCr,[19] this scenario is plausible but not evident, because the reduction of α-KL mRNA levels was at most 50% in the diabetic patients and mouse model of diabetes.

To confirm the scenario, we investigated UCa/UCr levels in α-KL$^{+/-}$ mice. Half reduction of α-KL expression *per se* did not lead to hypercalciuria in α-KL$^{+/-}$ mice. However, when we induced diabetes by STZ injection in α-KL$^{+/-}$ and α-KL$^{+/+}$ mice, diabetes-induced increment of UCa/UCr levels was significantly larger in α-KL$^{+/-}$ mice than in

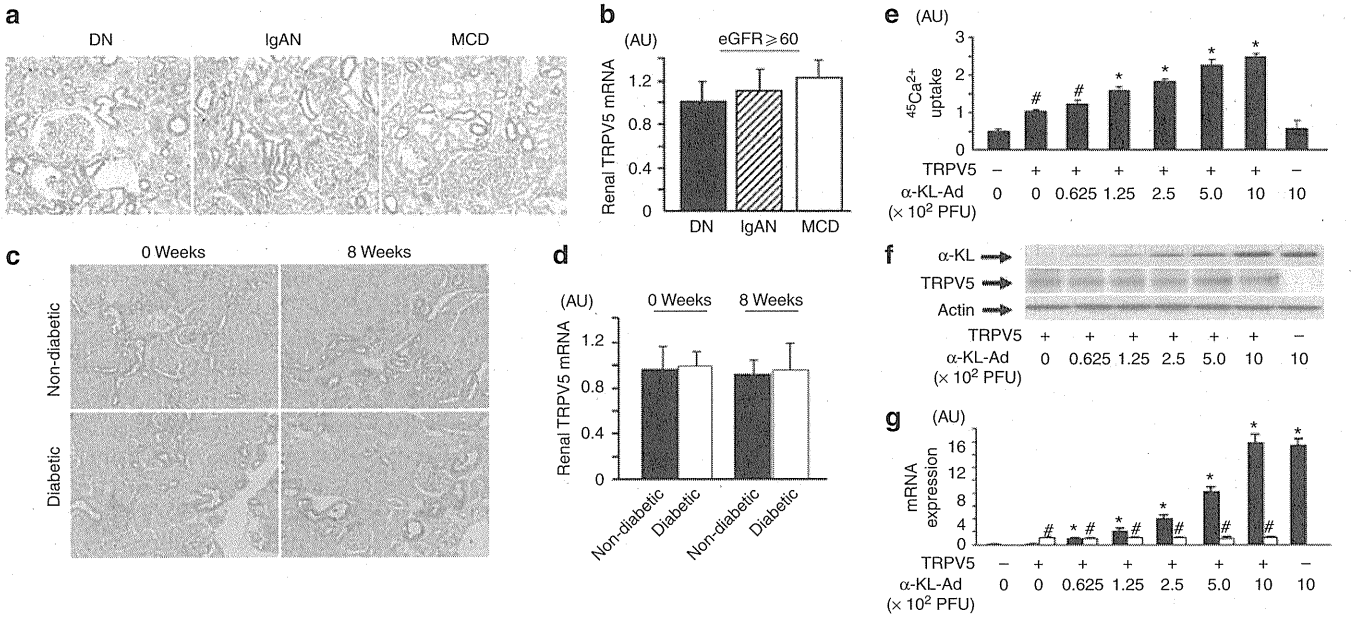


**Figure 7 | The effect of α-KL expression levels on the activity of transient receptor potential vanilloid calcium channel subtype 5 (TRPV5).** (**a**) Representative immunoperoxidase staining for TRPV5 in renal biopsy sections from human patients with diabetic nephropathy (DN), IgA nephropathy (IgAN), and minimal change disease (MCD). (**b**) Renal TRPV5 mRNA expression levels in DN (black bars), IgAN (striped bars), and MCD (white bars). (**c**) Representative immunoperoxidase staining for TRPV5 in kidney specimens from the indicated mice. (**d**) Renal TRPV5 mRNA expression levels in STZ diabetic (black bars) and nondiabetic (white bars) mice. (**e**) $^{45}Ca^{2+}$ uptake in HEK293 cells transfected with adenovirus carrying the *α-KL* gene (α-KL-Ad) or *Lac Z* gene as control, at the indicated doses, with or without TRPV5 expression. (**f**) Western blotting and (**g**) mRNA expression levels of α-KL (black bars) and TRPV5 (white bars) in the indicated HEK293 cells. Data are shown as means ± s.e.m. for each group. Original magnification, × 100. Student's *t*-test was used to compare groups. $^{\#}P<0.05$, vs. HEK293 cells without TRPV5 and α-KL gene transfected; $^{*}P<0.05$, vs. HEK293 cells transfected with TRPV5 and Lac Z.

α-$KL^{+/+}$ mice within 2 weeks after the establishment of diabetes mellitus, even when DN-related further decline of α-KL expression was not detected (Figure 6). Therefore, the increased UCa/UCr levels in the diabetic patients and mouse model of diabetes result from not only some diabetes-related changes such as glomerular hyperfiltration of calcium but also the 50% reduction in renal α-KL mRNA expression. Thus, hypercalciuria in the early stages of DN is at least partly due to α-KL loss in DCT.

Recently, evidence has accumulated that TRPV5 and $Na^+/K^+$-ATPase were carriers to mediate the activity of α-KL on calcium excretion in the DCTs.[14,18,24] Our *in vitro* analyses showed that, in HEK293 cells transfected with both TRPV5 and α-KL, calcium uptake was significantly increased in proportion to the α-KL expression, indicating that the reduction of α-KL expression may be related to a reduced abosorption of calcium via TRPV5 channels in the DCTs. This effect could reduce the capacity for calcium reabsorption in the DCTs to a level insufficient to meet the demand of the glomerular hyperfiltrated calcium in DN, which would in turn lead to more increasing urinary calcium excretion as α-KL expression levels decline. However, the other molecules including $Na^+/K^+$-ATPase may mediate the activity of α-KL on calcium excretion in the kidney, and further studies will be needed to more precisely clarify these underlying mechanism.

In conclusion, α-KL expression levels in the DCTs are decreased in the early stages of DN, which may affect urinary excretion of calcium in early DN.

## MATERIALS AND METHODS

### Study population

This study evaluated 74 patients with DN who manifested microalbuminuria, macroalbuminuria, and/or overt proteinuria, 90 patients diagnosed with IgAN by renal biopsy, and 26 patients with MCD. Spot urine and serum samples were collected between 0600 and 1000 h after a 10-h overnight fast. Serum levels of total protein, albumin, creatinine, calcium, inorganic phosphate, and glucose, as well as urinary levels of protein, creatinine, calcium, and inorganic phosphate, were measured in all patients. Serum $1,25(OH)_2$ vitamin $D_3$ levels were measured by radioimmunoassay, and serum i-PTH levels were measured by ECLIA (SRL, Tokyo, Japan). Serum fibroblast growth factor 23 concentrations were measured by using an ELISA kit (Kainos laboratories, Tokyo, Japan). eGFR was calculated by the creatinine-based Modification of Diet in Renal Disease Study equation.[25] Patient characteristics are listed in Table 1. In this study population, we evaluate renal α-KL expression levels in 31 patients with DN who had undergone renal biopsy, 31 patients with IgAN, and 7 patients with MCD. Renal biopsy had been performed in patients, whose amount of urinary protein was over 0.5 g/day. The patient characteristics of this subset used to evaluate renal α-KL expression are listed in Supplementary Table online. All clinical study protocols were approved by our institutional ethics committee (No. 2002-009, Nara Medical University Ethics

Committee). Written informed consent was obtained in all cases from either the patient or his or her family members.

### Animal studies

C57BL/6 mice, originally obtained from Japan Clea (Tokyo, Japan), and α-KL$^{+/-}$ mice[15] were housed under specific pathogen-free conditions in the Animal Research Institute of Nara Medical University. Diabetes was induced in both adult male C57BL/6 mice and α-KL$^{+/-}$ mice at 8 weeks of age by intraperitoneal injections of STZ (200 mg/kg) as previously reported.[26] Mice were individually housed in metabolic cages to obtain 24-h urine collections before killing. Commercial kits were used to measure concentrations of urine creatinine and calcium (Creatinine-Test and Calcium E-Test Wako, Wako, Wako Pure Chemical Industries, Osaka, Japan), as well as albumin (Albuwell M, Exocell, Philadelphia, PA). All procedures involving mice were performed in accordance with the National Institutes of Health guidelines for the care and use of live animals and were approved by the Nara Medical University Animal Care Committee.

### Immunohistochemical studies

α-KL was immunohistochemically labeled using KM2076 antibody (1:50 dilution; a kind gift of Kyowa Hakko Kogyo);[27] human type I collagen was labeled using mouse anti-human collagen type I monoclonal antibodies (1:500 dilution; MP Biomedicals, LLC, Solon, OH); TRPV5 was labeled using rabbit anti-rat TRPV5 polyclonal antibodies (1:100 dilution; Alpha Diagnostic International, San Antonio, TX) in sections from human renal biopsy specimens and murine kidneys. Human CD31, a marker of PTCs, was labeled using mouse anti-human CD31 monoclonal antibodies (1:100 dilution; Dako, Glostrup, Denmark). After primary antibody staining, labeling was visualized using a Dako Envison Kit. The number of CD31-positive PTCs within the confines of each of 10 random fields (delineated by a 1-cm$^2$ ocular grid viewed at $\times$ 100 magnification) was expressed as a mean per field. We also evaluated the mean percentages of each of 10 random fields positive for type I collagen by using an auto-analyzer.

### DNA constructs

The coding sequence of wild-type TRPV5 was amplified from mouse (strain C57BL/6) kidney cDNA and cloned into the pcDNA3 vector (TRPV5-pcDNA3 vector). The coding sequence of wild-type α-KL was amplified from mouse (strain C57BL/6) kidney cDNA, and recombinant adenoviral vector carrying *α-KL* gene (adeno-α-KL) was constructed using the Adeno-X expression system according to the manufacturer's protocol (Clontech laboratories, Mountain View, CA). All constructs were verified by DNA sequence analysis.

### Cell transfection and $^{45}Ca^{2+}$ uptake assay

HEK293 cells were transfected with TRPV5-pcDNA3 vector using the FuGENE HD transfection reagent according to the manufacturer's protocol (Roche, Mannheim, Germany), and cultured in Dulbecco's modified Eagle's medium containing 10% fetal bovine serum, and infected with adeno-α-KL and the control adeno-Lac Z, respectively, in a six-well plate. Two days after transfection, $^{45}Ca^{2+}$ (1 uCi/ml) uptake was performed as described previously.[28,29]

### Western blotting

Kidney and cell lysates were prepared using lysis buffer, and western blot analysis was performed as previously reported,[27,29] using specific antibodies, including monoclonal rat antibody for α-KL protein (KM2076)[27] (1:500 dilution) and polyclonal rabbit antibody for TRPV5 protein (1:100; Alpha Diagnostic International).

### RNA extraction, reverse transcription, and real-time RT-PCR

Total cellular RNA was extracted from human frozen renal biopsy specimens, murine renal cortex, or HEK293 cells, and first-strand cDNA was constructed as previously described.[30,31] For real-time PCR, 1 μl of each first-strand reaction product was amplified with appropriate primers and the corresponding fluorescent probes for human and murine α-KL (assay IDs: Hs00183100_m1, Mm00502002_m1) and TRPV5 (assay IDs: Hs00219765_m1, Mm01166029_m1), human β-actin (assay ID: Hs00242273_m1), or murine glyceraldehydes-3-phosphate dehydrogenase (assay ID: Mm99999915_m1). These probes were designed by the Applied Biosystems 'Assay-on-Demand' service (Foster City, CA). The ratios of human α-KL/β-actin mRNA, human TRPV5/β-actin mRNA, murine α-KL/glyceraldehydes-3-phosphate dehydrogenase mRNA, and murine TRPV5/glyceraldehydes-3-phosphate dehydrogenase mRNA were calculated for each sample.

### Statistical analysis

Statistical analyses were performed with the StatView 5.0 software (SAS Institute, Cary, NC). Numerical results were expressed as means ± s.d. Student's *t*-test was used for normally distributed variables. To compare groups, we used a one-way analysis of variance, followed by *post-hoc t*-test with Fisher-Protected Least Significant Differences adjustment. For variables with a skewed distribution, we used a Kruskal–Wallis analysis of variance by ranks with Bonferroni adjustment. The Pearson correlation coefficient was used to assess the relationships between renal α-KL mRNA expression levels and clinical and pathological parameters. Multiple regression analysis was performed to assess the combined influence of clinical variables on UCa/UCr among all patients with DN, IgAN, and MCD, who had undergone renal biopsy. Independent variables included levels of renal α-KL expression, serum $1,25(OH)_2$ vitamin $D_3$, serum i-PTH, corrected serum calcium, as well as eGFR and age. *P*-values less than 0.05 were considered to be significant.

### DISCLOSURE

All the authors declared no competing interests.

### ACKNOWLEDGMENTS

This work was supported in part by a research grant from the Ministry of Education and Science of Japan. We are indebted to Miss Aya Asano and Mrs Miyako Sakaida of Nara Medical University for their excellent technical assistance.

### SUPPLEMENTARY MATERIAL

**Figure S1.** Time course of urinary albumin to creatinine ratios (UACR) in diabetic (closed circles) and nondiabetic (open circles) mice.

**Figure S2.** Representative features of STZ-induced diabetic (a, b, c) and nondiabetic (d, e, f) mouse kidneys (periodic acid–methenamine–silver stain) at 0 weeks (a, d), 4 weeks (b, e), and 8 weeks (c, f) after the establishment of diabetes.

**Table S1.** Clinical characteristics of patients for renal α-KL expression analysis.

Supplementary material is linked to the online version of the paper at http://www.nature.com/ki

## REFERENCES


1. Raskin P, Stevenson MR, Barilla DE *et al.* The hypercalciuria of diabetes mellitus: its amelioration with insulin. *Clin Endocrinol (Oxf)* 1978; **9**: 329–335.
2. Anwana AB, Garland HO. Renal calcium and magnesium handling in experimental diabetes mellitus in the rat. *Acta Endocrinol (Copenh)* 1990; **122**: 479–486.
3. Lee CT, Lien YH, Lai LW *et al.* Increased renal calcium and magnesium transporter abundance in streptozotocin-induced diabetes mellitus. *Kidney Int* 2006; **69**: 1786–1791.
4. Ward DT, Yau SK, Mee AP *et al.* Functional, molecular, and biochemical characterization of streptozotocin-induced diabetes. *J Am Soc Nephrol* 2001; **12**: 779–790.
5. Vestergaard P. Discrepancies in bone mineral density and fracture risk in patients with type 1 and type 2 diabetes—a meta-analysis. *Osteoporos Int* 2007; **18**: 427–444.
6. Yamamoto M, Yamaguchi T, Yamauchi M *et al.* Diabetic patients have an increased risk of vertebral fractures independent of BMD or diabetic complications. *J Bone Miner Res* 2009; **24**: 702–709.
7. Guruprakash GH, Krothapalli RK, Rouse D *et al.* The mechanism of hypercalciuria in streptozotocin-induced diabetic rats. *Metabolism* 1988; **37**: 306–311.
8. Ohara N. Impaired intestinal active calcium absorption and reduction of serum 1alpha, 25(OH)2D3 in streptozotocin-induced diabetic pregnant rats with hypocalcemia in their fetuses. *Clin Exp Obstet Gynecol* 2000; **27**: 100–102.
9. Schedl HP, Christensen KK, Ronnenberg WC. Effects of diabetes on calcium uptake by rat brush border membrane vesicles. *Clin Exp Pharmacol Physiol* 1995; **22**: 272–276.
10. Friedman PA, Gesek FA. Cellular calcium transport in renal epithelia: measurement, mechanisms, and regulation. *Physiol Rev* 1995; **75**: 429–471.
11. Garland HO, Harris PJ, Morgan TO. Calcium transport in the proximal convoluted tubule and loop of Henle of rats made diabetic with streptozotocin. *J Endocrinol* 1991; **131**: 373–380.
12. Boland PS, Garland HO. Renal micropuncture study of the effects of D-glucose tubular calcium handling in the anaesthetized rat. *Exp Physiol* 1993; **78**: 175–181.
13. Kuro-o M, Matsumura Y, Aizawa H *et al.* Mutation of the mouse klotho gene leads to a syndrome resembling ageing. *Nature* 1997; **390**: 45–51.
14. Imura A, Tsuji Y, Murata M *et al.* alpha-Klotho as a regulator of calcium homeostasis. *Science* 2007; **316**: 1615–1618.
15. Takeshita K, Fujimori T, Kurotaki Y *et al.* Sinoatrial node dysfunction and early unexpected death of mice with a defect of klotho gene expression. *Circulation* 2004; **109**: 1776–1782.
16. Tsujikawa H, Kurotaki Y, Fujimori T *et al.* Klotho, a gene related to a syndrome resembling human premature aging, functions in a negative regulatory circuit of vitamin D endocrine system. *Mol Endocrinol* 2003; **17**: 2393–2403.
17. Urakawa I, Yamazaki Y, Shimada T *et al.* Klotho converts canonical FGF receptor into a specific receptor for FGF23. *Nature* 2006; **444**: 770–774.
18. Chang Q, Hoefs S, van der Kemp AW *et al.* The beta-glucuronidase klotho hydrolyzes and activates the TRPV5 channel. *Science* 2005; **310**: 490–493.
19. Alexander RT, Woudenberg-Vrenken TE, Buurman J *et al.* Klotho prevents renal calcium loss. *J Am Soc Nephrol* 2009; **20**: 2371–2379.
20. Mogensen CE. Glomerular filtration rate and renal plasma flow in short-term and long-term juvenile diabetes mellitus. *Scand J Clin Lab Invest* 1971; **28**: 91–100.
21. Mogensen CE, Christensen CK, Pedersen MM *et al.* Renal and glycemic determinants of glomerular hyperfiltration in normoalbuminuric diabetics. *J Diabet Complications* 1990; **4**: 159–165.
22. Bohle A, Mackensen-Haen S, Wehrmann M. Significance of postglomerular capillaries in the pathogenesis of chronic renal failure. *Kidney Blood Press Res* 1996; **19**: 191–195.
23. Bohle A, von Gise H, Mackensen-Haen S *et al.* The obliteration of the postglomerular capillaries and its influence upon the function of both glomeruli and tubuli. Functional interpretation of morphologic findings. *Klin Wochenschr* 1981; **59**: 1043–1051.
24. Cha SK, Ortega B, Kurosu H *et al.* Removal of sialic acid involving Klotho causes cell-surface retention of TRPV5 channel via binding to galectin-1. *Proc Natl Acad Sci USA* 2008; **105**: 9805–9810.
25. Imai E, Horio M, Nitta K *et al.* Modification of the Modification of Diet in Renal Disease (MDRD) Study equation for Japan. *Am J Kidney Dis* 2007; **50**: 927–937.
26. Usui HK, Shikata K, Sasaki M *et al.* Macrophage scavenger receptor-a-deficient mice are resistant against diabetic nephropathy through amelioration of microinflammation. *Diabetes* 2007; **56**: 363–372.
27. Kato Y, Arakawa E, Kinoshita S *et al.* Establishment of the anti-Klotho monoclonal antibodies and detection of Klotho protein in kidneys. *Biochem Biophys Res Commun* 2000; **267**: 597–602.
28. van de Graaf SF, Hoenderop JG, Gkika D *et al.* Functional expression of the epithelial Ca(2+) channels (TRPV5 and TRPV6) requires association of the S100A10-annexin 2 complex. *EMBO J* 2003; **22**: 1478–1487.
29. Lu P, Boros S, Chang Q *et al.* The beta-glucuronidase klotho exclusively activates the epithelial Ca2+ channels TRPV5 and TRPV6. *Nephrol Dial Transplant* 2008; **23**: 3397–3402.
30. Yoshimoto S, Nakatani K, Iwano M *et al.* Elevated levels of fractalkine expression and accumulation of CD16+ monocytes in glomeruli of active lupus nephritis. *Am J Kidney Dis* 2007; **50**: 47–58.
31. Nakatani K, Fujii H, Hasegawa H *et al.* Endothelial adhesion molecules in glomerular lesions: association with their severity and diversity in lupus models. *Kidney Int* 2004; **65**: 1290–1300.

BRIEF COMMUNICATION www.jasn.org

# Urinary FSP1 Is a Biomarker of Crescentic GN

Masayuki Iwano,*† Yukinari Yamaguchi,† Takaaki Iwamoto,‡ Kimihiko Nakatani,† Masaru Matsui,† Atsushi Kubo,† Yasuhiro Akai,† Toshio Mori,‡ and Yoshihiko Saito†

*Division of Nephrology, Department of General Medicine, Faculty of Medical Sciences, University of Fukui, Fukui 910-1193, Japan; and †Department of First Internal Medicine and ‡Radioisotope Research Center, Nara Medical University, Kashihara, Nara 634-8522, Japan

## ABSTRACT

Fibroblast-specific protein 1 (FSP1)–expressing cells accumulate in damaged kidneys, but whether urinary FSP1 could serve as a biomarker of active renal injury is unknown. We measured urinary FSP1 in 147 patients with various types of glomerular disease using ELISA. Patients with crescentic GN, with or without antinuclear cytoplasmic antibody–associated GN, exhibited elevated levels of urinary FSP1. This assay had a sensitivity of 91.7% and a specificity of 90.2% for crescentic GN in this sample of patients. Moreover, we found that urinary FSP1 became undetectable after successful treatment, suggesting the possible use of FSP1 levels to monitor disease activity over time. Urinary FSP1 levels correlated positively with the number of FSP1-positive glomerular cells, predominantly podocytes and cellular crescents, the likely source of urinary FSP1. Even in patients without crescent formation, patients with high levels of urinary FSP1 had large numbers of FSP1-positive podocytes. Taken together, these data suggest the potential use of urinary FSP1 to screen for active and ongoing glomerular damage, such as the formation of cellular crescents.

*J Am Soc Nephrol* 23: ●●●–●●●, 2012. doi: 10.1681/ASN.2011030229

Crescentic GN is a particularly aggressive type of kidney disease in which glomerular injury causes rapidly progressive GN.[1,2] Strong immunosuppressive therapy should be administered as early as possible in order to prevent irreversible kidney scarring.[3] The widespread use of assays for antinuclear cytoplasmic antibody (ANCA) has facilitated the clinical diagnosis of pauci-immune crescentic GN.[4,5] However, there have been few studies of biomarkers that could potentially serve to identify all forms of crescentic GN.

Fibroblast-specific protein 1 (FSP1) is one of the S100 calcium-binding proteins, a family of secreted and cytosolic proteins involved in a variety of biologic processes.[6–8] A large number of FSP1-expressing cells ($FSP1^+$ cells) accumulate in kidneys showing active renal damage.[9–11] In this study, we hypothesize that FSP1 secreted from $FSP1^+$ cells in the kidney should be detectable in urine samples. To test that idea and to clarify the significance of urinary FSP1 as a biomarker of active glomerular damage, we established two monoclonal antibodies for human FSP1 and developed a method for measuring urinary FSP1 levels using a sandwich-type ELISA. We then used that assay to assess urinary FSP1 excretion in cases of human GN.

Urinary FSP1 levels were measured in 147 patients with various types of glomerular disease (Figure 1A). In patients with ANCA-associated GN, urinary FSP1 levels were significantly higher (median, 3.71 $\mu$g/g of creatinine [first quartile, third quartile, 0.71, 5.07 $\mu$g/g of creatinine]) than in patients with IgA nephropathy (0.0 $\mu$g/g of creatinine [0.0, 0.98 $\mu$g/g of creatinine]; $P<0.001$), minimal-change nephrotic syndrome (0.0 $\mu$g/g of creatinine [0.0, 0.87 $\mu$g/g of creatinine]; $P<0.0001$), or membranous nephropathy (0.0 $\mu$g/g of creatinine [0.0, 0.0 $\mu$g/g of creatinine]; $P<0.0001$). Urinary FSP1 was not detectable in any of the healthy volunteers. In 56 patients with IgA nephropathy, the percentages of glomeruli showing cellular crescents, fibrocellular crescents, global sclerosis, and segmental sclerosis correlated positively with urinary FSP1 levels (Supplemental Table 1). A high level of urinary FSP1 (5.21 $\mu$g/g of creatinine) was also observed in one patient with FSGS showing a cellular variant.

Urinary FSP1 levels did not differ between patients with primarily cellular crescents or fibrocellular crescents, but urinary FSP1 was undetectable in five patients with fibrous crescents (Supplemental Figure 1). In five patients with IgA nephropathy and three patients with lupus nephritis, cellular or fibrocellular crescents were identified in more than 20% of glomeruli (20% crescent

Received March 2, 2011. Accepted September 8, 2011.

Published online ahead of print. Publication date available at www.jasn.org.

**Correspondence:** Dr. Masayuki Iwano, Division of Nephrology, Department of General Medicine, Faculty of Medical Sciences, University of Fukui, 23-3 Matsuokashimoaizuki, Eiheiji-cho, Yoshida-gun, Fukui 910-1193 Japan. Email: miwano@u-fukui.ac.jp

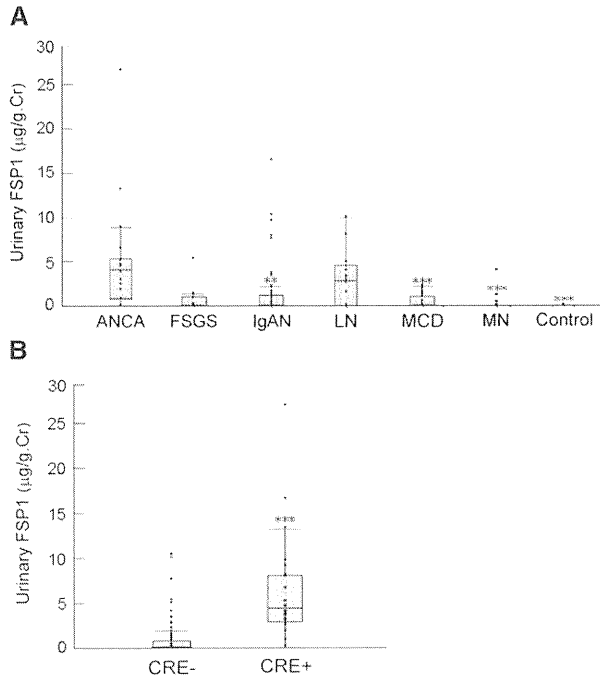


**Figure 1.** Elevation of urinary FSP1 in patients with ANCA nephritis and crescent formation. (A) Urinary FSP1 levels were measured in patients with ANCA-associated glomerulonephritis (ANCA), FSGS, IgA nephropathy (IgAN), lupus nephritis (LN), minimal-change nephrotic syndrome (MCD), or membranous nephropathy (MN). Urinary FSP1 levels were elevated in patients with ANCA and were undetectable in healthy volunteers (control). $^{**}P<0.001$ and $^{***}P<0.0001$ versus ANCA. Cr, creatinine. (B) Urinary FSP1 levels were significantly higher in patients with 20% crescent formation (CRE+) than those without it (CRE−).

formation). Given that urinary FSP1 levels were markedly elevated in these eight patients (5.93 μg/g of creatinine [3.45, 9.34 μg/g of creatinine), we divided the 147 study participants into two groups (with or without 20% crescent formation) and compared urinary FSP1 between these two groups. We found that urinary FSP1 levels were significantly higher in patients with 20% crescent formation than in those without it (4.48 μg/g of creatinine [2.91, 8.03 μg/g of creatinine] versus 0 μg/g of creatinine [0, 0.72 μg/g of creatinine]; $P<0.0001$) (Figure 1B).

To assess the diagnostic value of urinary FSP1 as a novel marker for crescent formation, we used receiver-operating characteristic curve analysis to determine a cut-off level for urinary FSP1 (Supplemental Figure 2) and made a 2×2 table. At FSP1 levels greater than 1.75 μg/g of creatinine, the assay had 90.2% specificity and 91.7% sensitivity for diagnosis in patients with 20% crescent formation. The positive and negative predictive values were 64.7% and 98.2%, respectively. We can also specifically select patients with 15% crescent formation by changing the FSP1 cut-off levels to greater than 5.0 μg/g of creatinine because both the specificity and the positive predictive value increased (to 98.3% and 86.7%, respectively), although the sensitivity decreased (to 43.3%).

The proteinuria level is a classic and valuable prognostic marker of CKD. However, proteinuria is not helpful for determining whether glomerular damage is ongoing. There have been a few studies of potential biomarkers for crescentic GN. Kanno and colleagues[12] showed that levels of urinary sediment podocalyxin are elevated in children with cellular crescents. Levels of urinary macrophage migration inhibitory factor and matrix metalloproteinase activity are reportedly higher in patients with crescentic GN and ANCA-associated GN than in healthy controls,[13,14] but the levels are not significantly higher than in patients with other glomerular diseases. By contrast, urinary FSP1 levels strongly correlated with the percentage of glomeruli showing cellular or fibrocellular crescent formation in patients with crescent formation, irrespective of the specific glomerular disease (Supplemental Figure 3). In addition, we confirmed a superiority of urinary FSP1 over other existing screening tests (C-reactive protein and serum creatinine) in diagnosing ANCA-negative crescentic GN (Supplemental Figure 4). These results suggest that urinary FSP1 may be useful for the diagnosis and management of all forms of crescentic GN.

We measured urinary FSP1 after therapy in six patients treated for ANCA-associated GN, three treated for lupus nephritis, and three treated for IgA nephropathy. All 12 patients had shown high levels of urinary FSP1 (FSP1 > 3.50 μg/g of creatinine) before therapy. However, urinary FSP1 was undetectable in 11 of those patients after successful treatment, which was judged according to the reduction of urinary protein levels and improvement of renal function. The 12th patient had lupus nephritis and continued to show proteinuria in the nephrotic range, a high titer of anti–double-stranded DNA, and severe hypocomplementemia. Moreover, urinary FSP1 levels continued to be high in this patient. This result suggests that FSP1 levels can be used as a follow-up marker.

We next measured FSP1 levels in serum samples obtained from 88 patients (14 patients with ANCA-associated GN, 38 with IgA nephropathy, 19 with minimal-change nephrotic syndrome, and 17 with membranous nephropathy) on the same day that urine samples were collected. We found that serum FSP1 levels were not elevated in the patients with ANCA-associated GN (Supplemental Figure 5), and there was no correlation between serum and urinary FSP1 levels (data not shown).

To investigate the origin of the urinary FSP1, we carried out an immunohistochemical analysis using an anti-FSP1 antibody. Figure 2A shows the three typical staining patterns. $FSP1^+$ cells accumulated

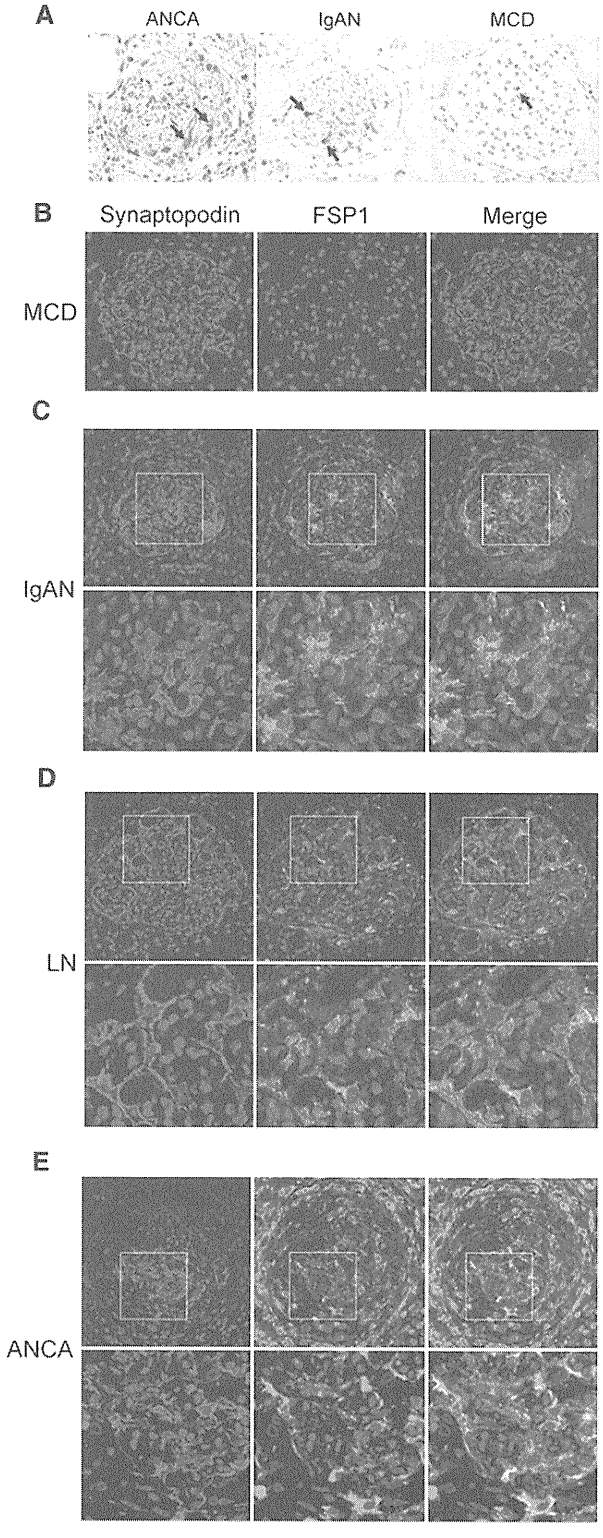


**Figure 2.** Increased expression of FSP1 in podocytes and cellular crescents. (A) Representative photomicrograph illustrating FSP1 expression within glomeruli. Large numbers of FSP1$^+$ cells accumulate in cellular crescents in patients with ANCA-associated glomerulonephritis (ANCA). FSP1$^+$ podocytes are localized on the outside of the glomerular basement membrane in a patient with IgA nephropathy (IgAN). FSP1$^+$ cells are rarely observed in a patient with minimal-change nephrotic syndrome (MCD). Arrows indicate FSP1$^+$ cells. (B–E) Representative immunofluorescence in renal biopsy specimens from patients with the following: (B) minimal-change nephrotic syndrome, (C) IgA nephropathy, (D) lupus nephritis (LN), and (E) ANCA. Cells expressing FSP1 (green) are clearly present within glomeruli from patients with IgA nephropathy, lupus nephritis, and ANCA. Merged images show co-localization of synaptopodin (red) and FSP1. Original magnification in upper panels, ×200. Lower panels are the high-power images of the boxed areas of the upper panels.

in cellular crescents in patients with ANCA-associated GN. FSP1$^+$ podocytes were observed in patients with IgA nephropathy. By contrast, FSP1$^+$ cell numbers in glomeruli were significantly lower in patients with minimal-change nephrotic syndrome (Figure 2, A and B). Moreover, as shown in Figure 2, C–E, dual immunofluorescence confirmed the presence of FSP1$^+$ podocytes in patients whose urinary FSP1 was higher than 1.75 $\mu$g/g of creatinine, irrespective of crescent formation. Indeed, FSP1$^+$ cell numbers and glomerular profile strongly correlated with urinary FSP1 levels (Figure 3). Taken together, these data suggest that FSP1$^+$ glomerular cells are the main source of urinary FSP1. In patients with no crescent formation, urinary FSP1 levels were significantly higher in those with more than six FSP1$^+$ podocytes than in those with fewer (Supplemental Figure 6). This finding suggests that both FSP1$^+$ podocytes and crescent-forming cells may contribute to urinary FSP1.

Identifying the origin of urinary FSP1 is difficult because elevated urinary FSP1 excretion could reflect enhanced intrarenal production, increased filtration, abnormal tubular reabsorption, or secretion from urinary cells that have detached from the renal structure. Serum FSP1 levels were not elevated in patients with crescent formation and did not correlate with urinary FSP1. Thus, urinary FSP1 excretion does not reflect increased systemic inflammation. Potential sites of FSP1 secretion into the urinary space are glomerular cells and tubular epithelial cells. The numbers of FSP1$^+$ tubular epithelial cells are much lower (<1.0/high-power field) than those of FSP1$^+$ glomerular cells, suggesting that glomerular cells are the main source of urinary

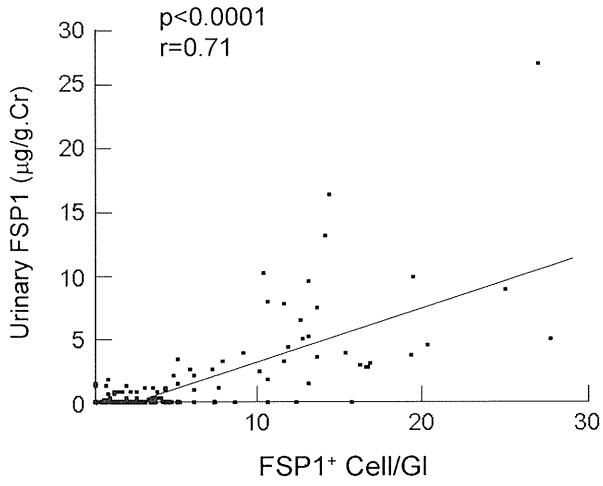


**Figure 3.** Urinary FSP1 levels are positively correlated with numbers of FSP1$^+$ cells/glomerular profile. Cr, creatinine; GI, glomerular profile.

FSP1. It was recently reported that FSP1 is secreted as a microparticle-like structure[15] and that podocytes are able to secrete proteins as microparticles through cellular shedding.[16] We further suggest that FSP1 secreted through microparticle shedding is not reabsorbed by tubular epithelial cells and is detected in urine samples. In addition, we previously demonstrated that more than 80% of detached podocytes express FSP1 in diabetic nephropathy, which suggests that some urinary FSP1 may be derived from detached podocytes or crescent cells. Because FSP1 was also produced by interstitial fibroblasts, the extent of renal fibrosis may have some effect on urinary FSP1 excretion. Urinary FSP1 levels weakly but significantly correlated with the extent of renal fibrosis evaluated according to the collagen type 1–positive area (Supplemental Figure 7). However, after adjustment for the number of FSP1$^+$ cells in the glomeruli, there was no association between the extent of renal fibrosis and urinary FSP1 levels.

Urinary FSP1 levels were significantly elevated in patients with high numbers of FSP1$^+$ podocytes, as well as in patients with 20% crescent formation. This finding suggests that the elevated urinary FSP1 levels are due in part to podocytes undergoing epithelial-mesenchymal transition and detaching from the glomerular basement membrane.[17–19] We previously reported that the appearance of FSP1 in podocytes of diabetic patients is associated with more severe clinical and pathologic findings of diabetic nephropathy, perhaps because of induction of podocyte detachment through an epithelial-mesenchymal transition–like phenomenon.[11] Urinary FSP1 may therefore be a novel risk factor for glomerular damage due to podocyte detachment, even in patients without crescent formation.

In summary, we established a novel ELISA system for measuring urinary FSP1, which appears to be a potentially useful biomarker for evaluating active glomerular damage, including crescent formation and the presence of FSP1$^+$ podocytes. Using this new biomarker clinically, we may be able to better identify patients who require hospitalization and urgent immunosuppressive therapy.

## CONCISE METHODS

### Production of Antihuman FSP1 Monoclonal Antibodies

An FSP1 expression vector was generated by cloning the full-length human *FSP1* gene into pET-49b(+) vector (Novagen, Darmstadt, Germany) carrying the GST-Tag and His-Tag sequences. BL21DE3-competent cells were then transformed using the FSP1 expression vector, after which protein expression was induced using isopropyl-$\beta$-D-thiogalactopyranoside (Takara Bio Inc., Shiga, Japan). The expressed fusion protein was purified by column chromatography using HisTrap HP columns (GE Healthcare, Tokyo, Japan), after which the GST-Tag and His-Tag were cleaved using human rhinovirus 3C protease (Novagen) to obtain the pure recombinant human FSP1 (rFSP1). The rFSP1 (50 $\mu$g/250 $\mu$l) was then emulsified in an equal volume of CFA (Difco Laboratories, Detroit, MI) and used as an immunogen.

To raise monoclonal antibodies, BALB/c mice (female, 7 weeks old) (Japan Clea, Tokyo, Japan) were intraperitoneally injected with the immunogen, and similar immunizations were carried out 2, 4, and 6 weeks later. One week after the fourth immunization, a booster injection of the immunogen without adjuvant was administered into the tail vein. Three days after the booster injection, the spleens were removed from the mice and dissociated by passage through 100-mesh steel gauze; the dissociated splenocytes ($2\times10^8$) were then fused with an equal number of myeloma cells in the presence of 50% polyethylene glycol 1500 (Roche Applied Science, Mannheim, Germany). The fused cells were then suspended in selective growth medium supplemented with 5% Briblone (Archport, Dublin, Ireland), distributed into the wells of 96-well culture plates ($2\times10^5$ hybrid cells/well), and cultured with periodic changes of the medium. The supernatants from wells containing hybridoma colonies were screened for the presence of specific antibodies using a direct ELISA, and the hybridoma cells from positive wells were cloned twice by limiting dilution. Each clone was then expanded in culture, after which the antibody-rich supernatants were concentrated by ammonium sulfate precipitation, dialyzed against PBS, and stored at −80°C.

Supernatants from 484 wells containing hybridoma cells were tested for antibodies. Using a direct ELISA and native PAGE, five were found to have preferential binding to rFSP1. From those we selected two clones that bound to rFSP1 with high titers (F1-2 and I11-23). Isotype analysis (Sterotec, Oxford, United Kingdom) revealed that F1-2 was of the IgG2a ($\kappa$) subclass, and I11-23 was of the IgG1 ($\kappa$) subclass. Through epitope mapping using PepSpots (JPT Peptide Technologies, Berlin, Germany), we confirmed that these two monoclonal antibodies bind to different epitopes: F1-2 recognizes the N-terminal end of

rFSP1, and I11-23 recognizes the EF hand calcium-binding domain. F1-2 was then biotinylated using NHS-LC-Biotin (Pierce Chemical, Rockford, IL), after which the efficacy of the surface biotinylation was confirmed using a 2-(4-hydroxyazobenzene) benzoic acid assay (Pierce Chemical).

### Development of a Sandwich ELISA

To construct a sandwich ELISA, we coated the bottom of each well of a polyvinyl chloride microtiter plate (Thermo Labsystems, Franklin, MA) with I11-23 (1 $\mu$g/50 $\mu$l PBS) and then incubated the plate overnight at 37°C. To construct a standard curve, urine samples and rFSP1 (from 1 to 64 ng/ml) were added to each well and incubated overnight at 4°C. After the incubation, the plates were washed five times with washing buffer (PBS containing 0.05% Tween-20). The biotinylated antibody (F1-2, 1 $\mu$g/100 $\mu$l) was then added to each well and incubated for 60 minutes at 37°C. The plates were again washed five times, after which horseradish peroxidase–conjugated streptavidin (Invitrogen, Tokyo, Japan) was added to each well and incubated for 60 minutes at 37°C. After washing, o-phenylenediamine dihydrochloride (0.2 mg/ml) (Sigma-Aldrich, St. Louis, MO) with 0.02% $H_2O_2$ was added and incubated for 30 minutes at 37°C. The colorimetric reaction was stopped by addition of 2 M $H_2SO_4$ (50 $\mu$l/well), and the adsorption at 492 nm was measured with a microplate reader. Urinary concentrations were adjusted for the creatinine concentration and expressed as micrograms per gram of creatinine. The intra-assay and interassay coefficients of variation were 3.5% and 8.4%, respectively. The detection limit of the test is 1 ng/ml.

### Patients and Sample Preparation

One hundred forty-seven patients (68 men and 79 women) with biopsy-proven glomerular disease were enrolled in this study after providing fully informed consent. This study was approved by our institutional review board. Patients with Henoch-Schönlein purpura nephritis, diabetes mellitus, neoplasia, viral hepatitis, amyloidosis, or other infections were excluded. The participants ranged from 16 to 89 years of age (mean age ± SD, 47.8±20.3 years). Before starting therapy, all patients were referred to the Department of Internal Medicine of Nara Medical University Hospital, and kidney biopsies were performed. Included were 19 patients with ANCA-associated GN, 10 with FSGS, 56 with IgA nephropathy, 13 with lupus nephritis, 29 with minimal-change nephrotic syndrome, and 20 with membranous nephropathy. Freshly voided urine samples were collected from each patient in the morning on the day renal biopsy was performed. Urine samples showing a urinary tract infection were excluded because of the possibility of nonspecific positivity. Macroscopic hematuria was also excluded because of the possibility of contamination by serum. Twenty-three age-matched healthy volunteers also provided urine samples. All samples were centrifuged for 10 minutes at 1500 *g* to remove any debris and were stored at −80°C before use.

### Immunohistochemistry

Renal biopsy specimens were fixed in 10% buffered formalin for 12 hours, dehydrated, embedded in paraffin, and sectioned according to standard procedures. The sections were then deparaffinized and incubated with proteinase K (0.4 mg/ml) for 5 minutes at room temperature for FSP1 staining or were incubated with 0.1% trypsin for 90 minutes at 37°C for collagen type 1 staining. The endogenous peroxidase activity was then blocked with 0.03% hydrogen peroxide, and nonspecific protein binding was blocked with 5% normal goat serum in PBS containing 2% BSA. The blocked sections were incubated for 60 minutes at room temperature with a primary rabbit polyclonal antihuman FSP1 antibody (1:5000 dilution) or with a primary rabbit polyclonal antihuman collagen type 1 antibody (1:500 dilution; Abcam, Cambridge, MA), after which the antibody was detected using a DAKO Envision+System peroxidase (diaminobenzidine) kit (DakoCytomation Inc., Carpinteria, CA). The sections were then counterstained with hematoxylin. The specificity of FSP1 staining was confirmed using control rabbit serum and by absorption of the anti-FSP1 antibody using an excess of rFSP1 protein. The area positively stained for collagen type 1 was calculated using AnalySIS image analysis software (Soft Imaging System, Munster, Germany).

Frozen sections of renal biopsy specimens were also stained for dual immunofluorescence microscopy. After the sections were fixed on glass slides in 4% paraformaldehyde for 15 minutes at 4°C, they were incubated for 60 minutes, first with goat polyclonal antihuman synaptopodin (P-19) antibody (1:500 dilution; Santa Cruz Biotechnology Inc., Santa Cruz, CA), and then with rabbit polyclonal antihuman FSP1 antibody (1:2000 dilution).[13] The sections were then washed three times with PBS and incubated for 30 minutes with DyLight 488-conjugated donkey anti-rabbit secondary antibody (1:800 dilution; Jackson ImmunoResearch Laboratories Inc., West Grove, PA) and a Cy3-conjugated donkey antigoat secondary antibody (1:1000 dilution; Jackson Immuno Research Laboratories Inc.). Finally, the sections were counterstained with 4′6-diamidine-2′- phenylindole dihydrochloride (Molecular Probes Inc., Eugene, OR) and viewed under a confocal microscope (Fluoview FV1000; Olympus, Tokyo, Japan).

### Statistical Analyses

Data were recorded as the median (25th percentile, 75th percentile), and $P<0.05$ was considered to represent a statistically significant difference. The Mann–Whitney *U* test was used for comparisons between two groups. The Kruskal–Wallis test with *post hoc* analysis using the Mann–Whitney test and adjustment of the *P* value using the Bonferroni method ($P<0.002$) was used to assess differences in clinical measures among more than three groups. Pearson correlation coefficients were used to assess relationships between urinary FSP1 and $FPS1^+$ cell number and glomerular profile. All analyses were performed using JMP 5.1 software (SAS Institute, Cary, NC). Sensitivity, specificity, and predictive values were calculated using receiver-operator characteristic curves and 2×2 tables.

## ACKNOWLEDGMENTS

We thank Ms. Fumika Kunda, Ms. Miyako Sakaida, and Ms. Aya Asano for excellent technical assistance and Dr. Keiichi Imagawa (Shionogi Co.) and Dr. Yoshiko Dohi (Nara Medical University) for helpful discussions.

This work was supported in part by Research Grant 21591036 to M.I. from the Ministry of Education and Science of Japan, a Grant-in-Aid for Diabetic Nephropathy from the Ministry of Health, Labour and Welfare of

Japan, and the Japan Science and Technology Agency.

## DISCLOSURES

None.

## REFERENCES


1. Morrin PA, Hinglais N, Nabarra B, Kreis H: Rapidly progressive glomerulonephritis. A clinical and pathologic study. *Am J Med* 65: 446–460, 1978
2. Couser WG: Rapidly progressive glomerulonephritis: Classification, pathogenetic mechanisms, and therapy. *Am J Kidney Dis* 11: 449–464, 1988
3. Bolton WK, Sturgill BC: Methylprednisolone therapy for acute crescentic rapidly progressive glomerulonephritis. *Am J Nephrol* 9: 368–375, 1989
4. Falk RJ, Jennette JC: ANCA small-vessel vasculitis. *J Am Soc Nephrol* 8: 314–322, 1997
5. Booth AD, Almond MK, Burns A, Ellis P, Gaskin G, Neild GH, Plaisance M, Pusey CD, Jayne DR Pan-Thames Renal Research Group: Outcome of ANCA-associated renal vasculitis: a 5-year retrospective study. *Am J Kidney Dis* 41: 776–784, 2003
6. Strutz F, Okada H, Lo CW, Danoff T, Carone RL, Tomaszewski JE, Neilson EG: Identification and characterization of a fibroblast marker: FSP1. *J Cell Biol* 130: 393–405, 1995
7. Iwano M, Plieth D, Danoff TM, Xue C, Okada H, Neilson EG: Evidence that fibroblasts derive from epithelium during tissue fibrosis. *J Clin Invest* 110: 341–350, 2002
8. Donato R: Intracellular and extracellular roles of S100 proteins. *Microsc Res Tech* 60: 540–551, 2003
9. Nishitani Y, Iwano M, Yamaguchi Y, Harada K, Nakatani K, Akai Y, Nishino T, Shiiki H, Kanauchi M, Saito Y, Neilson EG: Fibroblast-specific protein 1 is a specific prognostic marker for renal survival in patients with IgAN. *Kidney Int* 68: 1078–1085, 2005
10. Harada K, Akai Y, Yamaguchi Y, Kimura K, Nishitani Y, Nakatani K, Iwano M, Saito Y: Prediction of corticosteroid responsiveness based on fibroblast-specific protein 1 (FSP1) in patients with IgA nephropathy. *Nephrol Dial Transplant* 23: 3152–3159, 2008
11. Yamaguchi Y, Iwano M, Suzuki D, Nakatani K, Kimura K, Harada K, Kubo A, Akai Y, Toyoda M, Kanauchi M, Neilson EG, Saito Y: Epithelial-mesenchymal transition as a potential explanation for podocyte depletion in diabetic nephropathy. *Am J Kidney Dis* 54: 653–664, 2009
12. Kanno K, Kawachi H, Uchida Y, Hara M, Shimizu F, Uchiyama M: Urinary sediment podocalyxin in children with glomerular diseases. *Nephron Clin Pract* 95: c91–c99, 2003
13. Brown FG, Nikolic-Paterson DJ, Hill PA, Isbel NM, Dowling J, Metz CM, Atkins RC: Urine macrophage migration inhibitory factor reflects the severity of renal injury in human glomerulonephritis. *J Am Soc Nephrol* 13 [Suppl 1]: S7–S13, 2002
14. Sanders JS, Huitema MG, Hanemaaijer R, van Goor H, Kallenberg CG, Stegeman CA: Urinary matrix metalloproteinases reflect renal damage in anti-neutrophil cytoplasm autoantibody-associated vasculitis. *Am J Physiol Renal Physiol* 293: F1927–F1934, 2007
15. Forst B, Hansen MT, Klingelhöfer J, Møller HD, Nielsen GH, Grum-Schwensen B, Ambartsumian N, Lukanidin E, Grigorian M: Metastasis-inducing S100A4 and RANTES cooperate in promoting tumor progression in mice. *PLoS ONE* 5: e10374, 2010
16. Hara M, Yanagihara T, Kihara I, Higashi K, Fujimoto K, Kajita T: Apical cell membranes are shed into urine from injured podocytes: A novel phenomenon of podocyte injury. *J Am Soc Nephrol* 16: 408–416, 2005
17. Li Y, Kang YS, Dai C, Kiss LP, Wen X, Liu Y: Epithelial-to-mesenchymal transition is a potential pathway leading to podocyte dysfunction and proteinuria. *Am J Pathol* 172: 299–308, 2008
18. Bariety J, Hill GS, Mandet C, Irinopoulou T, Jacquot C, Meyrier A, Bruneval P: Glomerular epithelial-mesenchymal transdifferentiation in pauci-immune crescentic glomerulonephritis. *Nephrol Dial Transplant* 18: 1777–1784, 2003
19. Vogelmann SU, Nelson WJ, Myers BD, Lemley KV: Urinary excretion of viable podocytes in health and renal disease. *Am J Physiol Renal Physiol* 285: F40–F48, 2003


This article contains supplemental material online at http://jasn.asnjournals.org/lookup/suppl/doi:10.1681/ASN.2011030229/-/DCSupplemental.

Clin Exp Nephrol (2011) 15:321–330
DOI 10.1007/s10157-011-0434-0

REVIEW ARTICLE

# Clinicopathological insights into lupus glomerulonephritis in Japanese and Asians

**Hitoshi Yokoyama · Hiroshi Okuyama · Hideki Yamaya**

Received: 4 December 2010 / Accepted: 28 February 2011 / Published online: 25 March 2011


**Abstract** Lupus nephritis comprises a spectrum of glomerular, vascular, and tubulointerstitial lesions, which has significant racial variation in severity and manifestations. The current classification (ISN/RPS 2003) has been improved successfully for the categorization of lupus glomerulonephritis (LGN). On the basis of this classification, 480 Japanese cases revealed the following distribution: class I 3%, class II 16%, class III 13%, class IV-S 11%, class IV-G 41%, class V 16%, and class VI 1%. Class IV-G with chronicity tended to have the worst renal outcome. Nephrotic syndrome was a more frequent complication in class IV-S (50%), class IV-G (72%), and class V (56%), with poor renal and actuarial outcomes. With regard to therapy, treatment options including glucocorticoids alone or combined with antimetabolites (azathioprine, mizoribine, mycophenolate mofetil), calcineurin inhibitors (cyclosporine A, tacrolimus), or alkylating agents (intravenous cyclophosphamide injection) improved the outcome of LGN; however, there is no high-grade clinical evidence from Japan. Further studies are needed to resolve the clinicopathological problems of LGN, especially IV-S, IV-G, and pure membranous lupus nephritis in Japanese patients.

**Keywords** Lupus nephritis · ISN/RPS2003 classification · Race · Japanese · Asian

**Abbreviations**

| | |
|---|---|
| AZP | Azathioprine |
| CsA | Cyclosporine A |
| IVCY | Intravenous cyclophosphamide injection |
| LGN | Lupus glomerulonephritis |
| MLN | Membranous lupus nephritis |
| MZB | Mizoribine |
| MMF | Mycophenolate mofetil |
| Tac | Tacrolimus |

H. Yokoyama (✉) · H. Okuyama · H. Yamaya
Division of Nephrology, Kanazawa Medical University School of Medicine, Uchinada, Japan
e-mail: hyokoyama-npr@umin.ac.jp

## Introduction

Systemic lupus erythematosus (SLE) is a multisystem autoimmune disease with the characteristic development of autoantibodies to double-strand DNA and other nuclear antigens, as well as to membrane molecules such as phospholipids. About 20–50% of patients with lupus are reported to have abnormal urine test results in their early disease courses, and up to 60% of adults may go on to develop overt renal abnormalities [1]. Renal injuries in lupus nephritis comprise a spectrum of glomerular, vascular, and tubulointerstitial lesions, which may mainly result from circulating or in situ immune complex formation. Although lupus nephritis is strongly associated with substantial morbidity and early mortality, there is significant racial variation in the severity and manifestations of renal pathological lesions and clinical response to therapies [2–5]. The current classification (ISN/RPS 2003) has been improved successfully in terms of categorization and terminology for glomerular lesions in order to standardize the interpretation and reports of renal biopsies [6, 7].

In this review article, the current epidemiology, renal pathological diagnoses according to the ISN/RPS 2003 classification, clinical outcomes, and therapy of lupus nephritis in Japanese and other Asians are summarized.

## Epidemiology of lupus nephritis in Japan

The incidence rate of SLE in Okinawa (Japan) was 0.9 (1.6 for females, 0.4 for males) per 100,000 persons, and the prevalence of SLE from 1972 to 1991 increased from approximately 3.7 to 37.7 [8]. The number of SLE patients registered for a nationwide medical care study of intractable diseases in Japan reached 56,272 in 2008 (Fig. 1a).

With regard to lupus nephritis, nephritis has been reported in 31–65% of lupus cases in the USA and European countries, and in 45–86% of lupus cases in Japan. In the USA, Asian Americans, predominantly Chinese, were more likely to develop lupus nephritis than European Americans (hazard ratio 1.8, 95% confidence interval 1.6–1.9). The risk of lupus nephritis was greatest during the first few years after SLE diagnosis; however, the plateau in risk of lupus nephritis may occur up to 8 years following lupus diagnosis, and the nephritis-free survival of Asian Americans was only 33% [2]. In the cohort study of the Euro-Lupus Project, a cohort composed of 1,000 patients with SLE has been followed prospectively since 1991. Within the first 5 years (1990–1995), 222 cases (22.2%) had the complication of lupus nephritis; however, only 57 of 840 cases (6.8%) had nephritis in the next 5 years (1995–2000) [9]. From the registration data (J-RBR/J-KDR) of the Japanese Society of Nephrology for 2007–2009, 222 out of 5,703 renal biopsied cases, except for those with transplanted kidneys (3.5%), and 54 of 1,294 nephrotic cases (4.5%) were diagnosed with lupus nephritis. Even in the cohort of renal biopsied cases in the twenty first century, 54 of 222 (24.3%) Japanese patients with SLE had severe lupus nephritis.

From 1950 to 1980, lupus nephritis was strongly associated with early mortality, including in Japan; however, from 1980 to 2010, the outcome for SLE greatly improved to over 96% in terms of 5-year renal survival. The registered cases of end-stage renal failure (ESRF) due to lupus nephritis in The Annual Report of Regular Dialysis Treatment in Japan by the Patient Registration Committee, Japanese Society for Dialysis Therapy, numbered consistently around 300 per year (0.8–1.0% of total ESRF cases) in the most recent decade. On the other hand, the average age of ESRF patients who needed hemodialysis owing to lupus nephritis changed from 40 to 61 years old in the past 2 decades. Similarly,the prevalence of patients on hemodialysis due to lupus nephritis has increased from 285 with a mean age of 42 years old to 2,280 with a mean age of 58 years old in Japan since 1988 (Fig. 1b) [10].

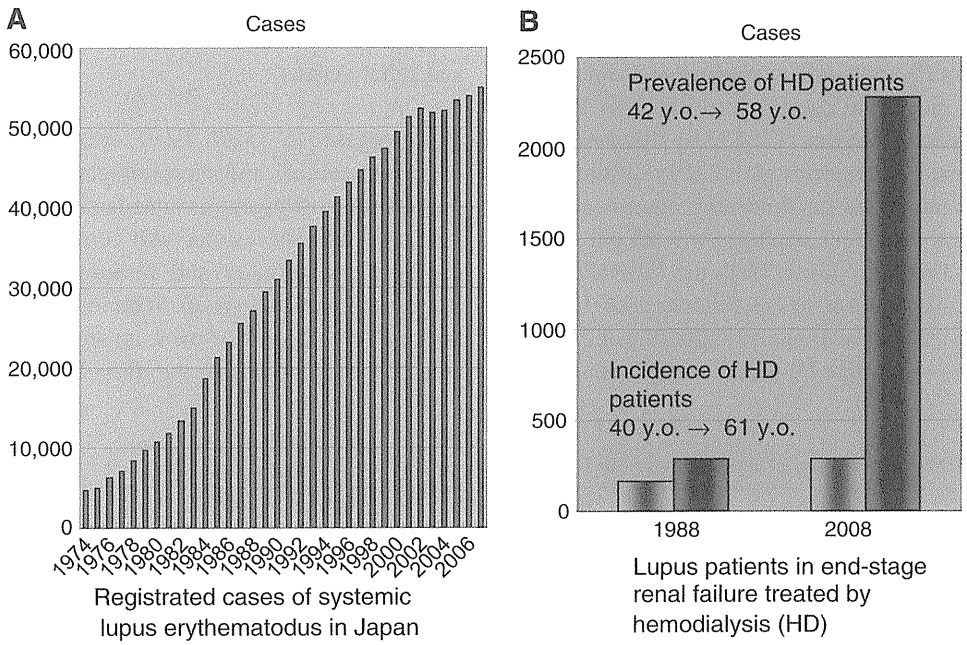


**Fig. 1** The prevalence of patients with systemic lupus erythematosus (SLE) and the incidence and prevalence of end-stage renal failure due to lupus nephritis from 1974 to 2008. **a** The SLE patients registered for a nationwide medical care study of intractable diseases in Japan numbered 56,272 by 2008. **b** Lupus patients with end-stage renal failure (ESRF) treated by hemodialysis (HD). The registered cases of ESRF by lupus nephritis numbered about 300 cases per year (0.8–1.0% of total ESRF cases) in the last decade. On the other hand, the average age of ESRF patients who needed HD owing to lupus nephritis changed from 40 to 61 years old in the past 2 decades. Similarly, the prevalence of patients who needed HD due to lupus nephritis increased from 285 with a mean age of 42 years old to 2,280 with a mean age of 58 years old in Japan from 1988 to 2008